MICHIGAN STATE UNIVERSITY

CYCLOTRON LABORATORY

LEVELS OF ^{56}Ni

H. NANN and W. BENENSON

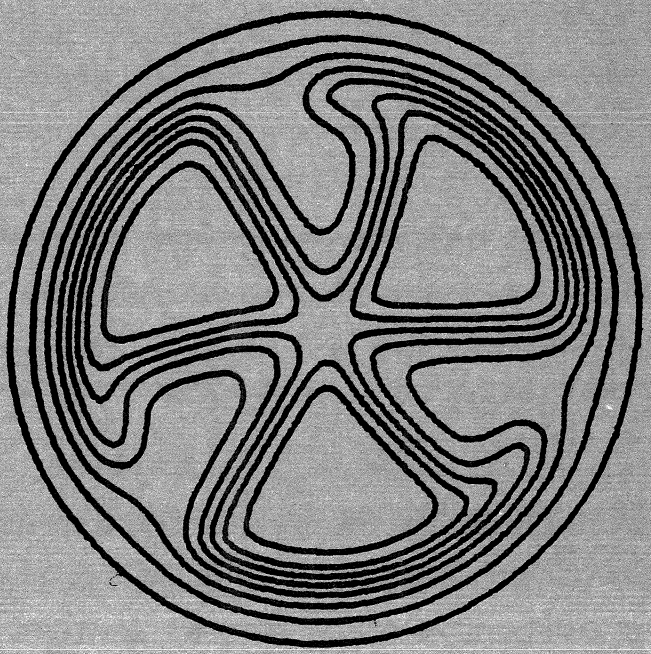

MSUCL-136

JULY 1974

Levels of ^{56}Ni*

H. Nann+ and W. Benenson

Cyclotron Laboratory and Department of Physics
Michigan State University, East Lansing, Michigan 48824

ABSTRACT

The $^{58}Ni(p,t)^{56}Ni$ reaction was studied at 40 and 45 MeV beam energy. An energy resolution of 10-25 keV permitted observation of 60 levels with excitation energy up to 10.5 MeV. Spin and parity are assigned to levels which were excited with characteristic angular distributions. These include 0^+ states at 3.95, 5.00, 6.44, 7.91, 9.92, 9.99 and 10.02 MeV.

[NUCLEAR REACTIONS: $^{58}Ni(p,t)^{56}Ni$, E_p=40.0 and 45.5 MeV; measured $\sigma(E_t,\theta)$; enriched target. ^{56}Ni deduced levels, L, J, π.]

*Work supported by the National Science Foundation.

+On leave of absence from the Institut für Kernphysik der J.W. Goethe Universität, Frankfurt/M, West Germany.

I. Introduction

In the shell-model description, ^{56}Ni is a doubly closed shell nucleus. Therefore the excitations and nature of levels in this nucleus are of considerable importance in nuclear structure calculations. The level structure of ^{56}Ni has been investigated by several authors with only two reactions, $^{58}Ni(p,t)^{56}Ni$[1,2] and $^{54}Fe(^3He,n)^{56}Ni$.[3-6] Since all these studies suffered from a lack of good energy resolution, some discrepancies exist even for low lying states. In the present paper these discrepancies are shown to arise from doublets only one of which had been previously resolved by a $^{54}F(He,n\gamma)^{56}Ni$ experiment.[7] As an example, in (p,t) experiments a spin-parity value of 4^+ was assigned to the level at 3.95 MeV whereas a value of 0^+ was found in the $(^3He,n)$ experiments. In order to resolve this type of discrepancy we measured the $^{58}Ni(p,t)^{56}Ni$ reaction with better energy resolution than had been previously obtained in studies of ^{56}Ni.

Angular distributions were obtained from 4° to 55° for approximately 60 resolved levels. A beam energy of 40 MeV was employed, at which energy the angular distributions displayed characteristic shapes for each L-transfer except for excitation energies greater than 6.5 MeV where only L=0 could be distinguishe This behavior is due to the low energy of the emitted tritons, which has been shown previously[8] to produce angular distributions which lack distinguishing features. The region of the T=2 state i ^{56}Ni (≃10 MeV) was repeated at 45.5 MeV beam energy to determine unambiguously the L-transfers in that region.

II. Experimental Procedure

The wire-counter plastic-scintillator combination[9] used in previous (p,t) experiments with the Michigan State University Cyclotron was adequate for most of the levels studied in the present experiment. This equipment provides excellent particle identification, but the approximately 1 mm spatial resolution corresponds to 25 keV which is larger than the spacing of many of the doublets in ^{56}Ni. For this reason close lying doublets required use of a silicon position-sensitive detector which permitted a spatial resolution about 0.5 mm. The wire counter data were taken in two passes; one from 0 to 6 MeV excitation energy, and the other from 5 to 11 MeV. The silicon detector covered only 700 keV excitation and was used for three regions; one around 4 MeV, the second near 5.7 MeV and the third in the 10 MeV region where the T=2 state is expected to lie. A composite spectrum from the wire and silicon detector is given in Fig. 1.

The targets used in the present experiments were ^{58}Ni metal either self-supporting or on an enriched ^{12}C backing. The thicknesses were 240 μg/cm^2 and 130 μg/cm^2, respectively. A monitor counter detected elastically scattered proton at 90° to normalize the data. The angle subtended by the spectrometer entrance aperature was 1° for forward angles (less than 20°) and for the angular region around 35° where the angular distributions are rapidly varying. At all other angles a 2° aperature was employed. The absolute cross section normalization was obtained by measuring the ground state transition with a thick natural Ni

foil which was weighed. The accuracy of the absolute cross section is about 15%.

Considerable attention was given to determining the excitation energies with good accuracy. The method, which was similar to that employed previously,[10] does not rely on the linearity of the detector. The magnetic field of the spectrograph was adjusted to put each peak of interest on the same location of the focal plane. The agreement with previous γ-ray work[7] when it exists, is excellent. This procedure was not employed for every state, and therefore the accuracies vary from 3 to 10 keV. However, all the states of particular importance were measured with the minimum error possible. This error was due to a variety of sources including uncertainties in the beam energy, target energy loss, centroid determination, angle determination and calibration reaction Q-value.

III. Results

The excitation energies of the levels observed in the present experiment are given in Table I. Also shown are the most recent of the previously published data on ^{56}Ni. Spin and parity assignments are indicated where they could be made. Values in parenthesis indicate the most likely choice. The absence of any assignment actually implies $J^\pi \neq 0^+$ since L=0 transitions are easily identified. In particular, note that there are four low lying doublets in ^{56}Ni with spacing from 25 to 70 keV. Below 6.3 MeV excitation none of the states resolved in the present experiments appear to be doublets with spacing greater

than 5 keV. Each of the spin assignments below 6.3 MeV excitation will be discussed in the following subsections. Except for the states with L=0 angular distributions, the levels above 6.3 MeV, when excited by the (p,t) reaction at 40 MeV, produce angular distributions without the characteristic features which can be related to the spin and the parity either by a DWBA calculation or comparison to levels with known spin values.

III.a. L=0 Transitions

Eight levels were observed to be excited by L=0 transitions. The excitation energies vary from 0 to 10.02 MeV, and therefore at 40 MeV bombarding energy the energy of the outgoing tritons varies from 26 to 16 MeV. This variation produces a considerable effect on the shape of the L=0 angular distributions as can be seen in Figs. 2(a) and 2(b). The main effect is on the first minimum which progressively disappears with high excitation energies. The intensities of the transitions vary considerably and are difficult to compare to each other because of the shape differences. The intensity ratios, which are given in Table II, vary according to which part of the angular distribution is used and will be discussed in a later section. One state near 7.25 MeV previously identified as 0^+ by Bruge and Leonard[2] is shown to be definitely not L=0 in the present experiment. The same is true for the four 0^+ states (6.0, 7.69, 9.75 and 10.25 MeV) observed by Fuchs et al.[6] None of these states shows an L=0 angular distribution as can be seen in Fig. 7.

The first attempt to locate the T=2 state in ^{56}Ni was hindered by a shape effect of the type described above. The experiment by Sherr et al.[11] was performed with apparatus similar to that described in the present paper, but the beam energy was 34 MeV. Three peaks with identically shaped angular distributions were observed in the region where the T=2 state is expected to lie. These shapes could not be unambiguously identified as L=0, and therefore it was not possible to determine whether the T=2 state was split into a doublet or triplet. In the mass region near A=56 several of the analog states are split into doublets which permits an interesting calculation involving the mixing due to a Coulomb off-diagonal matrix element. (See for example Dzubay et al.[12]) The existence of a triplet, however, can not be described with the same model. The present experiment at 40 MeV produced results very similar to those of Sherr et al. Three states displayed identically shaped distributions as can be seen in fig. 3(a), but they are still not unambiguous L=0. Therefore the experiment on the 10 MeV region of excitation energy was repeated at 45.5 MeV bombarding energy, and these data are presented in fig. 3(b). It is clear that there are three L=0 transitions, two with almost equal intensity and the third about four times bigger. Thus the approximate location of the T=2 state in ^{56}Ni is E_x=9.95 MeV. This is an average excitation for the three levels weighted by their cross section. However it is really not possible to assign definitely any T=2 strength to the higher lying doublet, and therefore the unperturbed energy may be as low as 9.92 MeV.

III.b. L=2 Transitions

Besides the first excited state, only two other levels can be shown to have L=2 angular distributons. These are shown in Fig. 4. The present data does not rule out or support the assignment of 2^+ to states near 6.24, 6.33, 6.57 and 7.43 MeV by Bruge and Leonard.[2] The assignments of Bruge and Leonard were made by finding the L-transfer of the DWBA calculation which fits the shape of the angular distribution best. This procedure has been found to be incapable of unambiguously distinguishing L-transfers which differ by one unit and in some cases even two units. To elucidate this problem the $^{56}Fe(p,t)^{54}Fe$ reaction was studied for states of known spin in the final nucleus. These shapes provided a much more reliable signature of L-transfer than the DWBA calculations, which fit quite poorly in some cases. The present data on ^{56}Ni were also very poorly fit by the DWBA calculations particularly at the most forward angles. Since the data of Bruge and Leonard did not include these forward angles or as many data points, they were therefore unable to observe this discrepancy between calculations and the experimental angular distributions. The present data do not rule out or support a 2^+ assignment by Fuchs et al.[6] to states at 8.08, 9.33, 9.45 and 10.82 MeV. The 8.08 MeV state did not appear in the (p,t) spectra.

III.c. L=4 Transitions

Five L=4 angular distributions were observed. These are shown in Fig. 5. The identification of this L-transfer is based on a comparison to $^{56}Fe(p,t)^{54}Fe$ at the same beam energy.

The transition to the 4^+ state in ^{54}Fe at 3.84 MeV has angular distribution essentially identical to the 3.923 MeV state in ^{56}Ni. The key features are the minimum near 41°, a second maximum at 50° and sharp fall off from 50° to 60°. L=2 angular distributions are similar in appearance but the minima, maxima and fall-off occur at different angles. A state identified by Bruge and Leonard at 5.48 MeV as 3^- by the procedure described above is much more likely to be 4^+ as can be seen in Fig. 5.

III.d. L=3 Transitions

There is one possible case of a state excited by an L=3 angular distribution. This assignment is based on the comparison to $^{56}Fe(p,t)^{54}Fe$ shown in Fig. 6. The 6.40 MeV 3^- state in ^{54}Fe is one of three 3^- states in that nucleus which all display the same shape for the angular distribution. Although the statistical accuracy of the data is good, the lack of a marked structure prevents an unambiguous assignment.

III.e. Other Transitions

Most of the states below 6.4 MeV which were not assigned an L-transfer are weakly populated and hence could be examples of unnatural parity states or states with $L \geq 4$. The 4.932 MeV state is an example of what is most likely an unnatural parity state. This angular distribution is shown in Fig. 7 along with an example of a probably L=6 for the 5.32 MeV state. The L=6 identification is the only one in this paper based on a DWBA calculation. The calculation does reproduce the data almost exactly, however, no L=6 angular distributions were available in

nearby nuclei for comparison purposes. Above 6.4 MeV, very few states show marked structure in their angular distributions because of the low energy of the outgoing tritons. However two states at 7.25 and 7.80 MeV have identical shapes and are possibly excited with L=1. The effect of the low triton energy even obscures the L-transfer to the strong and well-known 2^+, T=1 states which lies at 7.43 MeV.

IV. Discussion

The character of some of the 0^+ states discussed above can be investigated by comparing $^{58}Ni(p,t)^{56}Ni$ and $^{54}Fe(^3He,n)^{56}Ni$ cross sections to that level. For example in $(^3He,n)$ the 0^+ state at 3.95 MeV is excited strongly (with about 50% of the ground state) whereas in (p,t) it is weakly excited (with about 3% of the ground state transition). This can be understood as a 2p-2h state in the simplest shell model picture with ^{58}Ni as $(2p_{3/2})^2_{J=0}$ outside a closed $f_{7/2}$ shell and ^{54}Fe as two holes in the $f_{7/2}$ shell. A 2p-2h state in ^{56}Ni would then be strong in $(^3He,n)$ and weak in (p,t) since the transfer strength of a $2p_{3/2}$ pair is stronger than of a $1f_{7/2}$ pair by a factor of about six.

The 0^+ state at 5.01 MeV is weakly excited in $(^3He,n)$ (10% of the ground state) and very weakly excited in (p,t) (1% of the ground state). Such behavior is an indication of a predominantly 4p-4h state, which is excited by small admixtures to the simple wave functions if a direct one-step process is responsible for the transition.

Transitions to 0^+ states can also be considered within the framework of the pairing vibrational model as was investigated originally by Bohr[13] and Nathan.[14] They identified the T=0, 1 and 2 components of the pairing vibration mode having one addition and one removal quantum with the 0^+ states at 6.66, 7.91 and 9.92 MeV. According to this model, the intensity ratios for $^{58}Ni(p,t)^5$ reaction to this triplet of levels should be 2:3:1. Experimentally the ratio is found to be 0.6:1.3:1 with errors of about 25%. The error in the intensity ratios could be improved by doing the experiment at a high enough energy that the shapes of the angular distributions would become more similar. Q-value effects would also be reduced by performing the experiment at a higher beam energy.

The transitions to the 0^+ states at 3.95 and 5.01 MeV are not described by the pairing vibrational model. Bohr has suggested that the 5.00 MeV state is formed with two addition and two removal quanta. The 3.95 MeV state is very difficult to understand within the framework of the pairing vibrational model since only by neglecting its presence can the T(T+1) splitting rule be applied with success to the spacing of the 6.66, 7.91 and 9.92 MeV T=0, 1 and 2 states.

There exist several shell-model studies[15,16] and one Hartree-Fock[17] calculation for ^{56}Ni. None of these calculations considered a low lying 0^+ state at 3.95 MeV, and hence it is difficult to make any comparisons. A nucleus like ^{56}Ni which has the same closed neutron and proton shells in lowest order is very difficult to calculate successfully. The problems are similar to that encountered in ^{16}O but are intensified by the difficulty of

handling the $f_{7/2}$ shell. In addition to the new levels found in the present experiment some γ-ray transition strengths are now known,[7,18] so it is perhaps a suitable time to recalculate ^{56}Ni in the shell model.

FIGURE CAPTIONS

Fig. 1--Composite triton spectrum of the $^{58}Ni(p,t)^{56}Ni$ reaction at $\theta_{Lab}=14°$.

Fig. 2(a) and (b)--Angular distributions for levels excited by L=0 transfers in the $^{58}Ni(p,t)^{56}Ni$ reaction.

Fig. 3--L=0 angular distributions for levels in ^{56}Ni around 10 MeV of excitation energy at a bombarding energy of (a) 40.0 MeV and (b) 45.5 MeV.

Fig. 4--Angular distributions for levels excited by L=2 transfers in the $^{58}Ni(p,t)^{56}Ni$ reaction.

Fig. 5--Angular distributions of $^{58}Ni(p,t)^{56}Ni$ transitions characteristic of L=4 transfer.

Fig. 6--Angular distributions for levels excited by L=3 transfers in the $^{56}Fe(p,t)^{54}Fe$ and $^{58}Ni(p,t)^{56}Ni$ reactions.

Fig. 7--Angular distributions of miscellaneous $^{58}Ni(p,t)^{56}Ni$ transitions.

REFERENCES

1. W. G. Davies, J. E. Kitching, W. McLatchie, D. G. Montague, K. Ramavatram, and N. S. Chant, Phys. Lett. 27B, 363(1968).
2. G. Bruge, and R. F. Leonard, Phys. Rev. C2, 220(1970).
3. R.P.J. Winsborrow, and B.E.F. Macefield, Nucl. Phys. A182, 481(1972).
4. D. Evers, W. Assmann, K. Rudolph, and S. J. Skorka, Nucl. Phys. A198, 268(1972).
5. W. P. Alford, R. A. Lindgren, and D. Elmore, Phys. Lett. 42B, 60(1972).
6. H. Fuchs, K. Grabisch, D. Hilscher, U. Jahnke, H. Kluge, T. G. Masterson, and H. Morgenstern, Phys. Lett. 49B, 447 (1974).
7. P. Schneider, A. Nagel, K.H. Bodenmiller, and S. Buhl, Z. Physik 253, 309(1972).
8. S. W. Cosper, H. Brunnader, J. Cerny, and R. L. McGrath, Phys. Lett. 25B, 324(1967).
9. H. Nann, W. Benenson, W. A. Lanford, and B. H. Wildenthal, Phys. Rev. in press.
10. E. Kashy, W. Benenson, I. D. Proctor, P. Hauge, and G. Bertsch, Phys. Rev. C7, 2251(1973).
11. R. Sherr, W. Benenson, E. Kashy, D. Bayer and I. Proctor, Bull. Am. Phys. Soc. 16, 509(1971).

12. T. G. Dzubay, R. Sherr, F. D. Becchetti, Jr., and D. Dehnhard, Nucl. Phys. A142, 488(1970).
13. A. Bohr, Symp. on Nuclear Structure, Dubna (IAEA, Vienna, 1968), p. 179.
14. O. Nathan, ibid., p. 191.
15. S.S.M. Wong, and W. G. Davies, Phys. Lett. 28B, 77 (1968).
16. G. Oberlechner, and J. Richert, Nucl. Phys. A191, 577 (1972).
17. G. Do Dang, and J. A. Rabbat, Can. J. Phys. 51, 737 (1973).
18. N. Schulz, J. Chevallier, B. Haas, J. Richert, and M. Toulemonde, Phys. Rev. C8, 1779(1972).

Table I. Summary of states in ^{56}Ni. All energies are in MeV with errors in parenthesis in keV.

present work		$(p,t)^a$		$(p,t)^b$		$(^3He,n)^c$		$(^3He,n)^d$		$(^3He,n\gamma)^e$		$(^3He,n)^f$	
E_x	J^π	E_x	J^π	E_x	J^π	E_x	J^π	E_x	J^π	E_x	J^π	E_x	J^π
0	0^+	0	0^+	0	0^+	0	0^+	0	0^+	0	0^+	0	0^+
2.702(3)	2^+	2.697	2^+	2.64	2^+	2.66	2^+	2.54	2^+	2.702	2^+	2.70	2^+
3.923(3)	4^+	3.956	4^+	3.90	4^+	3.90				3.925	0^+		
3.952(3)	0^+					3.96	0^+	3.95	0^+	3.958	4^+	3.95	0^+
4.932(3)	$(3^+,5^+)$												
5.002(3)	0^+	5.000	0^+	4.95	0^+	5.00	(0^+)			5.011	0^+	5.01	0^+
5.316(3)	6^+	5.339	6^+										
5.351(3)	2^+			5.33	(2^+)	5.40	(2^+)			5.352	(2^+)	5.32	2^+
5.490(3)	(4^+)	5.483	3^-										
5.679(3)	(6^+)												
5.799(3)													
5.985(3)	(2^+)	5.989	(4^+)	5.90	(4^+)								
6.011(3)												6.0	0^+
6.236(3)		6.222	(2^+)										
6.327(3)	(3^-)	6.318	2^+										
												6.38	2^+
6.436(3)	4^+	6.419	4^+	6.38	4^+								
6.517(10)													

Table I.--Cont.

present work		$(p,t)^a$		$(p,t)^b$		$(^3He,n)^c$		$(^3He,n)^d$		$(^3He,n\gamma)^e$		$(^3He,n)^f$	
E_x	J^π	E_x	J^π	E_x	J^π	E_x	J^π	E_x	J^π	E_x	J^π	E_x	J^π
6.572(10)		6.554	(2^+)										
6.662(6)	0^+	6.644	0^+	6.58	0^+			6.50	0^+	6.660	0^+	6.62	0^+
6.730(8)													
7.025(10)		7.021		7.000								7.06	
7.144(6)		7.170	1^-	7.12	1^-							7.12	
7.250(8)	(1^-)	7.289	0^+										
7.433(8)		7.455	2^+	7.42	2^+					7.440	2^+	7.44	2^+
7.576(6)		7.567	3^-	7.56	3^-								
7.670(8)		7.653	$(1^-,2^+)$									7.69	0^+
7.801(10)	(1^-)	7.788											
7.913(5)	0^+	7.912	0^+	7.92	0^+	7.92	0^+	7.95	0^+	7.908	0^+	7.91	0^+
												8.08	
8.143(10)													
8.479(10)				8.48	2^+								
												8.52	2^+
8.575(10)													
8.674(8)		8.654				8.64	2^+	8.65	$(1^-,0^++2^+)$			8.69	2^+

Table I.--Cont.

present work		(p,t)[a]		(p,t)[b]		(^{3}He,n)[c]		(^{3}He,n)[d]		(^{3}He.nγ)[e]		(^{3}He,n)[f]	
E_x	J^π	E_x	J^π	E_x	J^π	E_x	J^π	E_x	J^π	E_x	J^π	E_x	J^π
8.796(6)	4^+	8.771											
8.870(12)		8.896										8.86	
9.008(6)												9.00	
9.042(8)													
9.109(8)													
9.154(10)													
9.235(12)													
9.310(10)												9.33	2^+
9.450(8)												9.45	2^+
9.596(6)													
9.676(6)													
												9.72	
9.740(5)													
9.756(5)												9.75	0^+
9.824(3)													
9.917(3)	0^+					9.96	0^+	10.01	0^+			9.94	0^+
9.994(3)	0^+												

Table I.--Cont.

present work		(p,t)[a]		(p,t)[b]		(^{3}He,n)[c]		(^{3}He,n)[d]		(^{3}He,nγ)[e]		(^{3}He,n)[f]	
E_x	J^π	E_x	J^π	E_x	J^π	E_x	J^π	E_x	J^π	E_x	J^π	E_x	J^π
10.021(3)	0^+												
10.055(3)													
10.095(5)													
10.150(5)													
10.250(6)												10.25	0^+
10.331(10)													
10.377(10)													
10.428(8)													
10.655(10)												10.65	
10.785(15)						10.77							
10.854(10)												10.82	2^+
												10.95	
11.055(15)													
												11.3	
												11.5	
												11.80	2^+
												12.30	

a) Ref. 2 b) Ref. 1 c) Ref. 4 d) Ref. 3 e) Ref. 7 f) Ref. 6

Table II. L=0 transition strengths

E_x (MeV)	based on 4°-8°	40°-50°
0	100	100
3.95	3	3
5.01	1	2
6.66	7	5
7.91	15	9
9.92	8	3
9.99	2	1
10.02	2	1

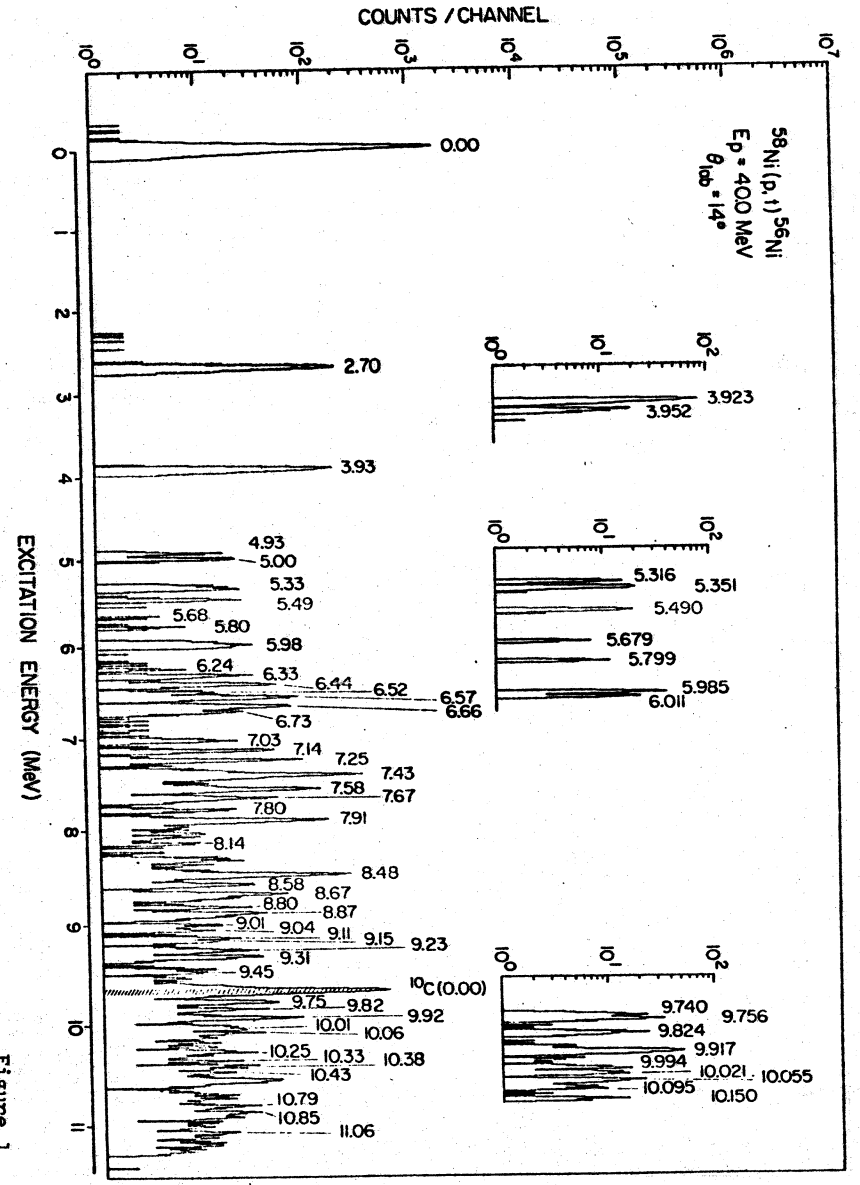

Figure 1

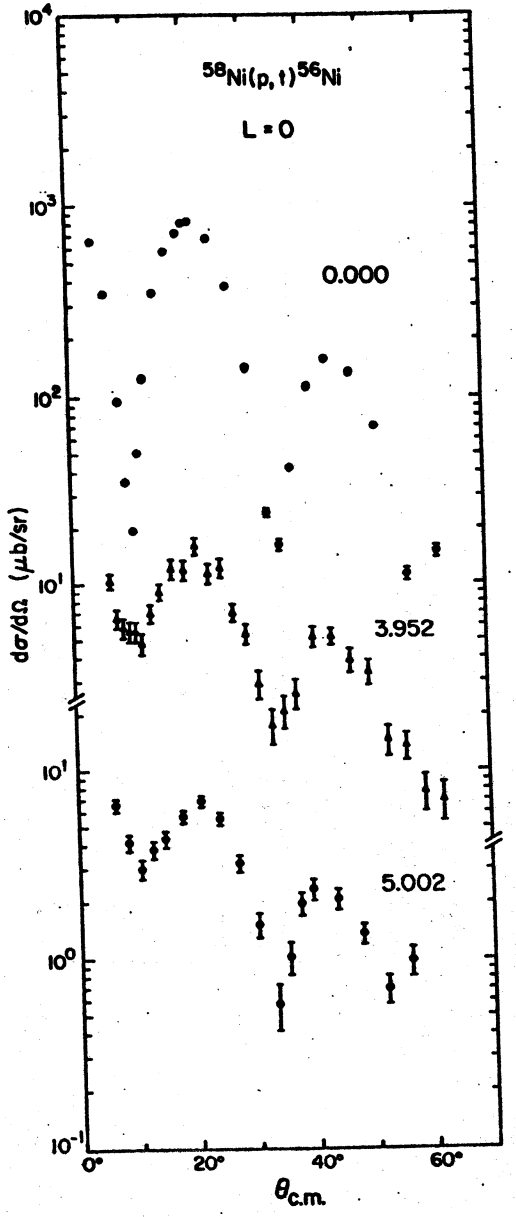

Figure 2 (a)

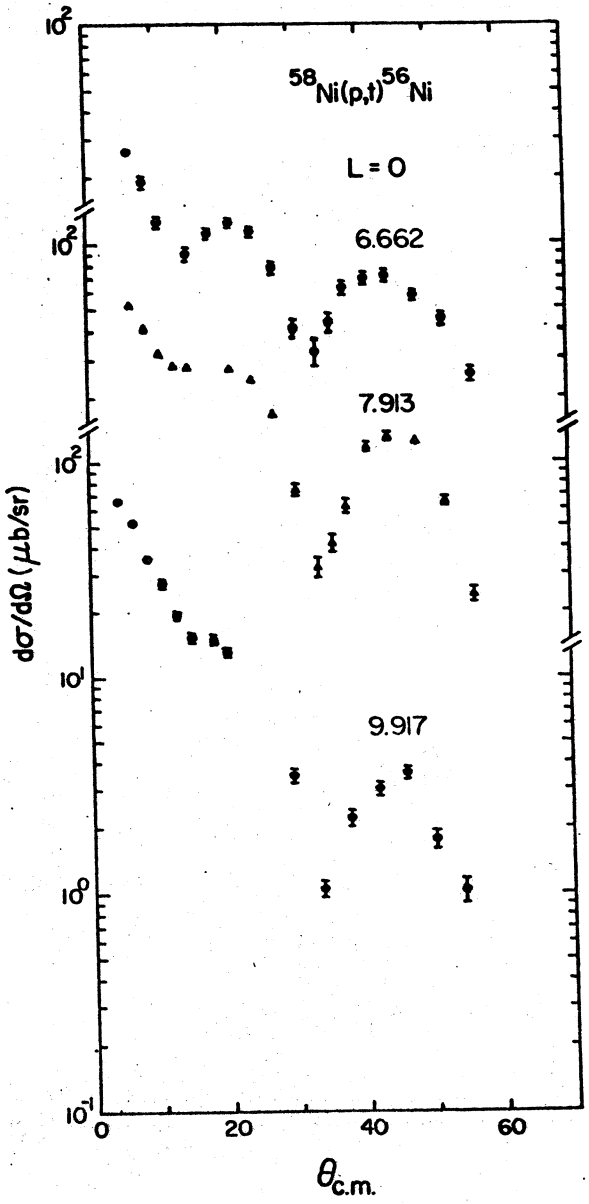

Figure 2 (b)

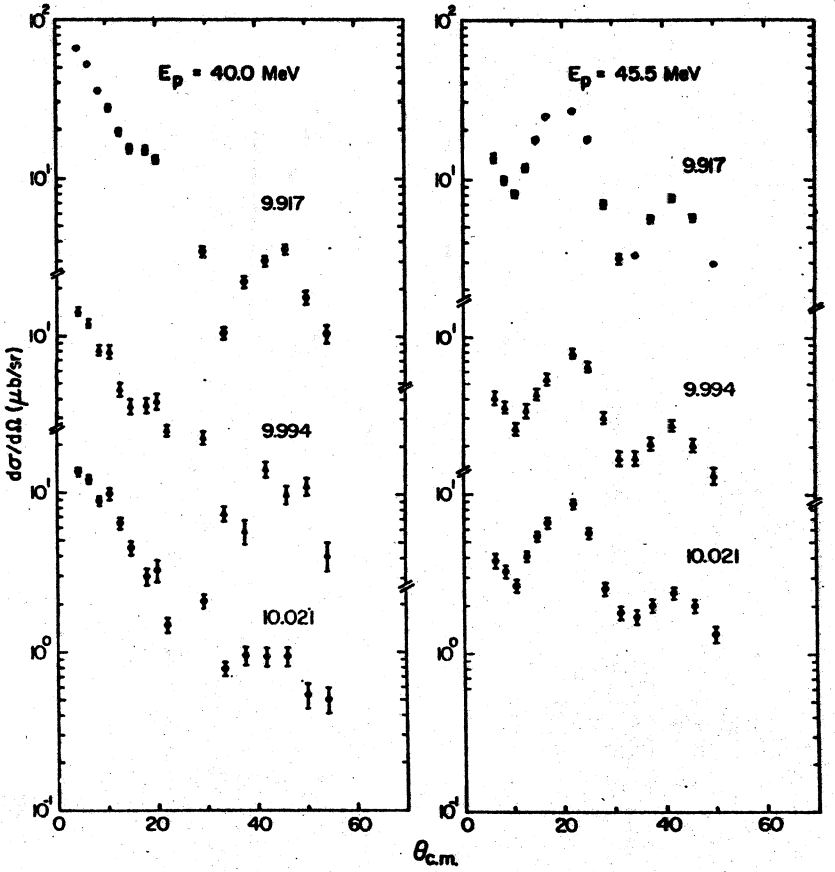

Figure 3

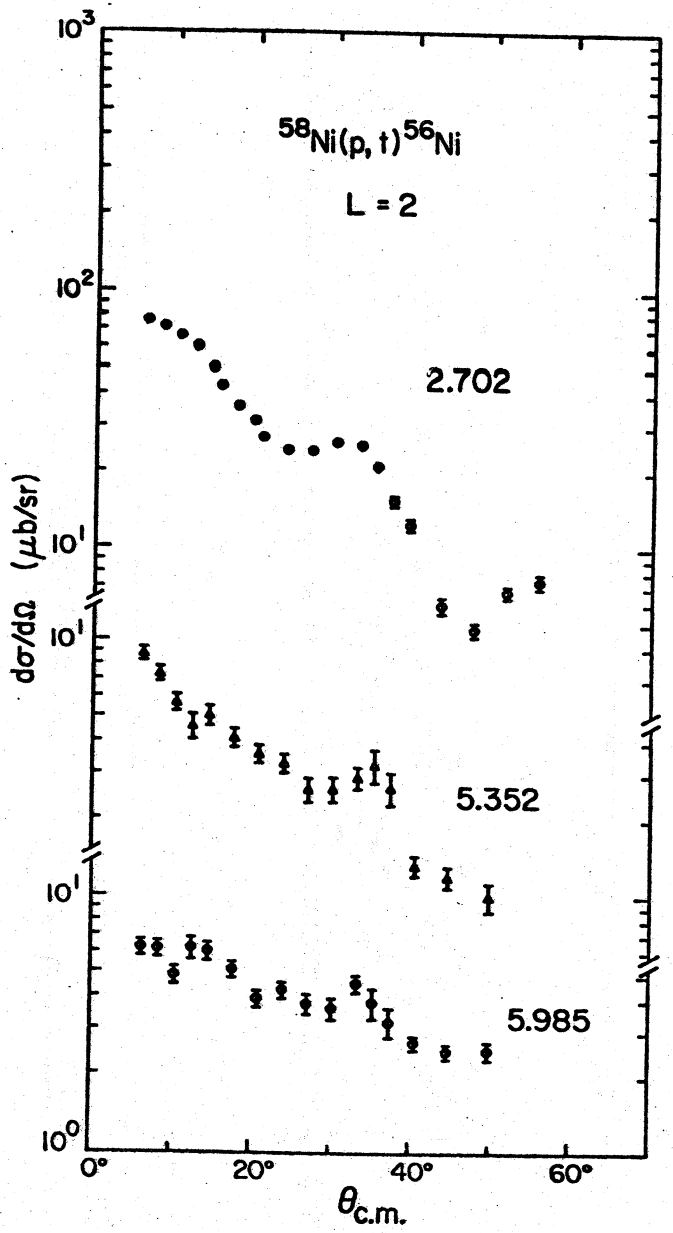

Figure 4

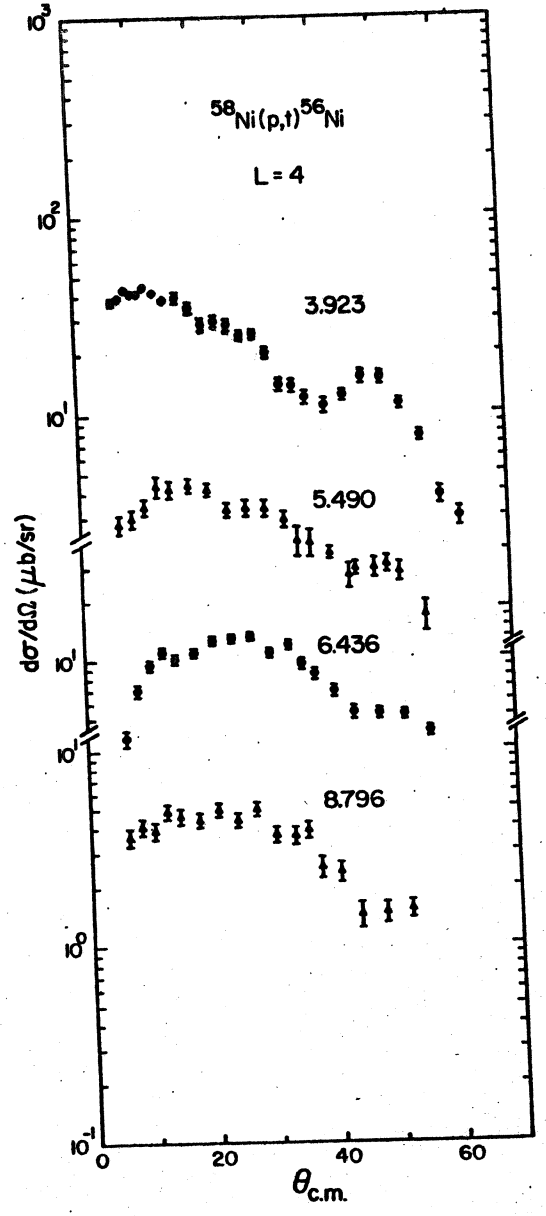

Figure 5

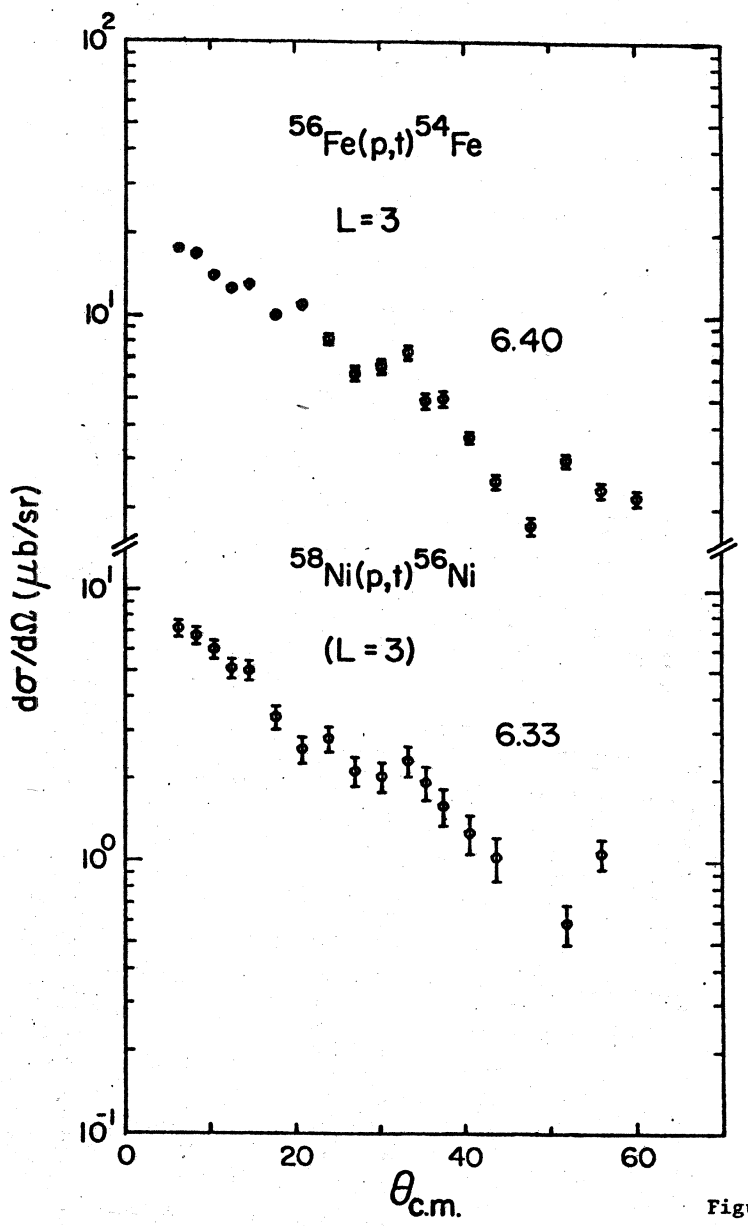

Figure 6

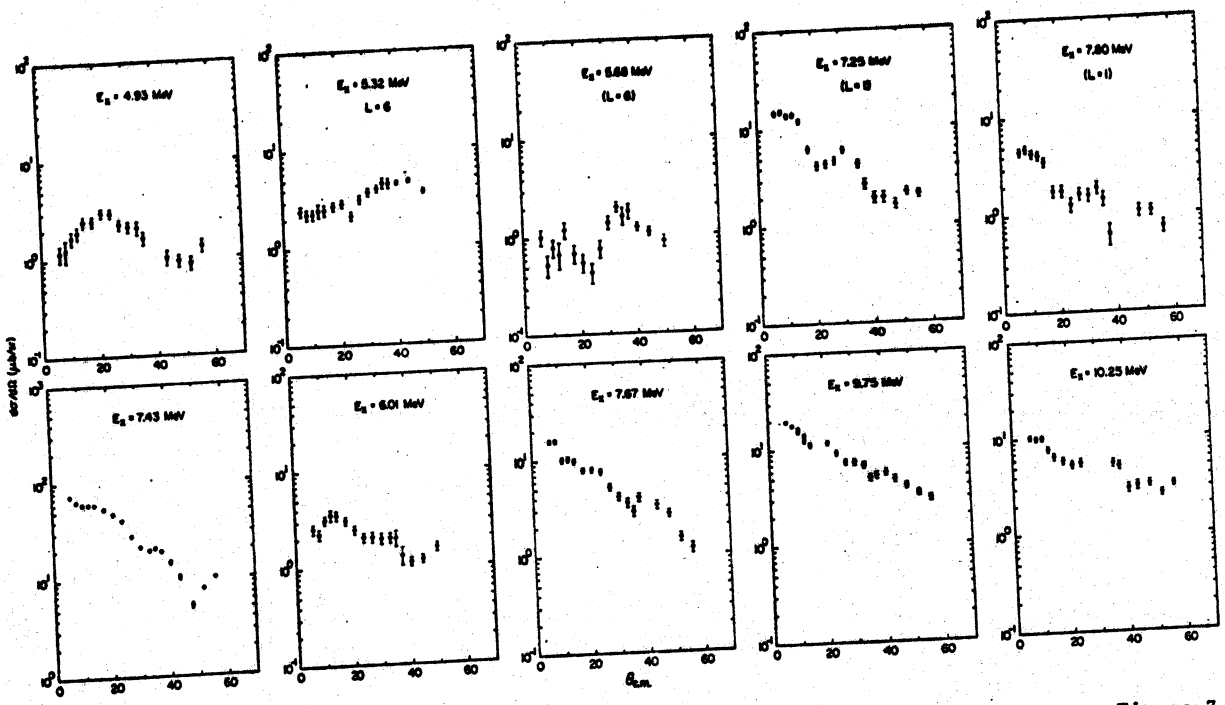
E_x = 4.93 MeV
E_x = 5.32 MeV
L = 6
E_x = 5.68 MeV
(L = 6)
E_x = 7.25 MeV
(L = 8
E_x = 7.80 MeV
(L = 1)
E_x = 7.43 MeV
E_x = 6.01 MeV
E_x = 7.67 MeV
E_x = 9.75 MeV
E_x = 10.25 MeV
$d\sigma/d\Omega$ (μb/sr)
$\theta_{c.m.}$

Figure 7